

Observation and Spin-Parity Determination of the $X(1835)$ in $J/\psi \rightarrow \gamma K_S^0 K_S^0 \eta$

M. Ablikim¹, M. N. Achasov^{9,f}, X. C. Ai¹, O. Albayrak⁵, M. Albrecht⁴, D. J. Ambrose⁴⁴, A. Amoroso^{48A,48C}, F. F. An¹, Q. An^{45,a}, J. Z. Bai¹, R. Baldini Ferroli^{20A}, Y. Ban³¹, D. W. Bennett¹⁹, J. V. Bennett⁵, M. Bertani^{20A}, D. Bettoni^{21A}, J. M. Bian⁴³, F. Bianchi^{48A,48C}, E. Boger^{23,d}, I. Boyko²³, R. A. Briere⁵, H. Cai⁵⁰, X. Cai^{1,a}, O. Cakir^{40A,b}, A. Calcaterra^{20A}, G. F. Cao¹, S. A. Cetin^{40B}, J. F. Chang^{1,a}, G. Chelkov^{23,d,e}, G. Chen¹, H. S. Chen¹, H. Y. Chen², J. C. Chen¹, M. L. Chen^{1,a}, S. J. Chen²⁹, X. Chen^{1,a}, X. R. Chen²⁶, Y. B. Chen^{1,a}, H. P. Cheng¹⁷, X. K. Chu³¹, G. Cibinetto^{21A}, H. L. Dai^{1,a}, J. P. Dai³⁴, A. Dbeysi¹⁴, D. Dedovich²³, Z. Y. Deng¹, A. Denig²², I. Denysenko²³, M. Destefanis^{48A,48C}, F. De Mori^{48A,48C}, Y. Ding²⁷, C. Dong³⁰, J. Dong^{1,a}, L. Y. Dong¹, M. Y. Dong^{1,a}, S. X. Du⁵², P. F. Duan¹, E. E. Eren^{40B}, J. Z. Fan³⁹, J. Fang^{1,a}, S. S. Fang¹, X. Fang^{45,a}, Y. Fang¹, L. Fava^{48B,48C}, F. Feldbauer²², G. Felici^{20A}, C. Q. Feng^{45,a}, E. Fioravanti^{21A}, M. Fritsch^{14,22}, C. D. Fu¹, Q. Gao¹, X. Y. Gao², Y. Gao³⁹, Z. Gao^{45,a}, I. Garzia^{21A}, C. Geng^{45,a}, K. Goetzen¹⁰, W. X. Gong^{1,a}, W. Gradi²², M. Greco^{48A,48C}, M. H. Gu^{1,a}, Y. T. Gu¹², Y. H. Guan¹, A. Q. Guo¹, L. B. Guo²⁸, Y. Guo¹, Y. P. Guo²², Z. Haddadi²⁵, A. Hafner²², S. Han⁵⁰, Y. L. Han¹, X. Q. Hao¹⁵, F. A. Harris⁴², K. L. He¹, Z. Y. He³⁰, T. Held⁴, Y. K. Heng^{1,a}, Z. L. Hou¹, C. Hu²⁸, H. M. Hu¹, J. F. Hu^{48A,48C}, T. Hu^{1,a}, Y. Hu¹, G. M. Huang⁶, G. S. Huang^{45,a}, H. P. Huang⁵⁰, J. S. Huang¹⁵, X. T. Huang³³, Y. Huang²⁹, T. Hussain⁴⁷, Q. Ji¹, Q. P. Ji³⁰, X. B. Ji¹, X. L. Ji^{1,a}, L. L. Jiang¹, L. W. Jiang⁵⁰, X. S. Jiang^{1,a}, X. Y. Jiang³⁰, J. B. Jiao³³, Z. Jiao¹⁷, D. P. Jin^{1,a}, S. Jin¹, T. Johansson⁴⁹, A. Julin⁴³, N. Kalantar-Nayestanaki²⁵, X. L. Kang¹, X. S. Kang³⁰, M. Kavatsyuk²⁵, B. C. Ke⁵, P. Kiese²², R. Kliemt¹⁴, B. Kloss²², O. B. Kolcu^{40B,i}, B. Kopf⁴, M. Kornicer⁴², W. Kühn²⁴, A. Kupsc⁴⁹, J. S. Lange²⁴, M. Lara¹⁹, P. Larin¹⁴, C. Leng^{48C}, C. Li⁴⁹, C. H. Li¹, Cheng Li^{45,a}, D. M. Li⁵², F. Li^{1,a}, G. Li¹, H. B. Li¹, J. C. Li¹, Jin Li³², K. Li¹³, K. Li³³, Lei Li³, P. R. Li⁴¹, T. Li³³, W. D. Li¹, W. G. Li¹, X. L. Li³³, X. M. Li¹², X. N. Li^{1,a}, X. Q. Li³⁰, Z. B. Li³⁸, H. Liang^{45,a}, Y. F. Liang³⁶, Y. T. Liang²⁴, G. R. Liao¹¹, D. X. Lin¹⁴, B. J. Liu¹, C. X. Liu¹, F. H. Liu³⁵, Fang Liu¹, Feng Liu⁶, H. B. Liu¹², H. H. Liu¹⁶, H. H. Liu¹, H. M. Liu¹, J. Liu¹, J. B. Liu^{45,a}, J. P. Liu⁵⁰, J. Y. Liu¹, K. Liu³¹, K. Liu³⁹, K. Y. Liu²⁷, L. D. Liu³¹, P. L. Liu^{1,a}, Q. Liu⁴¹, S. B. Liu^{45,a}, X. Liu²⁶, X. X. Liu⁴¹, Y. B. Liu³⁰, Z. A. Liu^{1,a}, Zhiqiang Liu¹, Zhiqing Liu²², H. Loehner²⁵, X. C. Lou^{1,a,h}, H. J. Lu¹⁷, J. G. Lu^{1,a}, R. Q. Lu¹⁸, Y. Lu¹, Y. P. Lu^{1,a}, C. L. Luo²⁸, M. X. Luo⁵¹, T. Luo⁴², X. L. Luo^{1,a}, M. Lv¹, X. R. Lyu⁴¹, F. C. Ma²⁷, H. L. Ma¹, L. L. Ma³³, Q. M. Ma¹, T. Ma¹, X. N. Ma³⁰, X. Y. Ma^{1,a}, F. E. Maas¹⁴, M. Maggiore^{48A,48C}, Y. J. Mao³¹, Z. P. Mao¹, S. Marcello^{48A,48C}, J. G. Messchendorp²⁵, J. Min^{1,a}, T. J. Min¹, R. E. Mitchell¹⁹, X. H. Mo^{1,a}, Y. J. Mo⁶, C. Morales Morales¹⁴, K. Moriya¹⁹, N. Yu. Muchnoi^{9,f}, H. Muramatsu⁴³, Y. Nefedov²³, F. Nerling¹⁴, I. B. Nikolaev^{9,f}, Z. Ning^{1,a}, S. Nisar⁸, S. L. Niu^{1,a}, X. Y. Niu¹, S. L. Olsen³², Q. Ouyang^{1,a}, S. Pacetti^{20B}, P. Patteri^{20A}, M. Pelizaeus⁴, H. P. Peng^{45,a}, K. Peters¹⁰, J. Pettersson⁴⁹, J. L. Ping²⁸, R. G. Ping¹, R. Poling⁴³, V. Prasad¹, Y. N. Pu¹⁸, M. Qi²⁹, S. Qian^{1,a}, C. F. Qiao⁴¹, L. Q. Qin³³, N. Qin⁵⁰, X. S. Qin¹, Y. Qin³¹, Z. H. Qin^{1,a}, J. F. Qiu¹, K. H. Rashid⁴⁷, C. F. Redmer²², H. L. Ren¹⁸, M. Ripka²², G. Rong¹, Ch. Rosner¹⁴, X. D. Ruan¹², V. Santoro^{21A}, A. Sarantsev^{23,g}, M. Savrié^{21B}, K. Schoenning⁴⁹, S. Schumann²², W. Shan³¹, M. Shao^{45,a}, C. P. Shen², P. X. Shen³⁰, X. Y. Shen¹, H. Y. Sheng¹, W. M. Song¹, X. Y. Song¹, S. Sosio^{48A,48C}, S. Spataro^{48A,48C}, G. X. Sun¹, J. F. Sun¹⁵, S. S. Sun¹, Y. J. Sun^{45,a}, Y. Z. Sun¹, Z. J. Sun^{1,a}, Z. T. Sun¹⁹, C. J. Tang³⁶, X. Tang¹, I. Tapan^{40C}, E. H. Thorndike⁴⁴, M. Tiemens²⁵, M. Ullrich²⁴, I. Uman^{40B}, G. S. Varner⁴², B. Wang³⁰, B. L. Wang⁴¹, D. Wang³¹, D. Y. Wang³¹, K. Wang^{1,a}, L. L. Wang¹, L. S. Wang¹, M. Wang³³, P. Wang¹, P. L. Wang¹, S. G. Wang³¹, W. Wang^{1,a}, X. F. Wang³⁹, Y. D. Wang¹⁴, Y. F. Wang^{1,a}, Y. Q. Wang²², Z. Wang^{1,a}, Z. G. Wang^{1,a}, Z. H. Wang^{45,a}, Z. Y. Wang¹, T. Weber²², D. H. Wei¹¹, J. B. Wei³¹, P. Weidenkaff²², S. P. Wen¹, U. Wiedner⁴, M. Wolke⁴⁹, L. H. Wu¹, Z. Wu^{1,a}, L. G. Xia³⁹, Y. Xia¹⁸, D. Xiao¹, Z. J. Xiao²⁸, Y. G. Xie^{1,a}, Q. L. Xiu^{1,a}, G. F. Xu¹, L. Xu¹, Q. J. Xu¹³, Q. N. Xu⁴¹, X. P. Xu³⁷, L. Yan^{45,a}, W. B. Yan^{45,a}, W. C. Yan^{45,a}, Y. H. Yan¹⁸, H. J. Yang³⁴, H. X. Yang¹, L. Yang⁵⁰, Y. Yang⁶, Y. X. Yang¹¹, H. Ye¹, M. H. Ye^{1,a}, M. H. Ye⁷, J. H. Yin¹, B. X. Yu^{1,a}, C. X. Yu³⁰, H. W. Yu³¹, J. S. Yu²⁶, C. Z. Yuan¹, W. L. Yuan²⁹, Y. Yuan¹, A. Yuncu^{40B,c}, A. A. Zafar⁴⁷, A. Zallo^{20A}, Y. Zeng¹⁸, B. X. Zhang¹, B. Y. Zhang^{1,a}, C. Zhang²⁹, C. C. Zhang¹, D. H. Zhang¹, H. H. Zhang³⁸, H. Y. Zhang^{1,a}, J. J. Zhang¹, J. L. Zhang¹, J. Q. Zhang¹, J. W. Zhang^{1,a}, J. Y. Zhang¹, J. Z. Zhang¹, K. Zhang¹, L. Zhang¹, S. H. Zhang¹, X. Y. Zhang³³, Y. Zhang¹, Y. N. Zhang⁴¹, Y. H. Zhang^{1,a}, Y. T. Zhang^{45,a}, Yu Zhang⁴¹, Z. H. Zhang⁶, Z. P. Zhang⁴⁵, Z. Y. Zhang⁵⁰, G. Zhao¹, J. W. Zhao^{1,a}, J. Y. Zhao¹, J. Z. Zhao^{1,a}, Lei Zhao^{45,a}, Ling Zhao¹, M. G. Zhao³⁰, Q. Zhao¹, Q. W. Zhao¹, S. J. Zhao⁵², T. C. Zhao¹, Y. B. Zhao^{1,a}, Z. G. Zhao^{45,a}, A. Zhemchugov^{23,d}, B. Zheng⁴⁶, J. P. Zheng^{1,a}, W. J. Zheng³³, Y. H. Zheng⁴¹, B. Zhong²⁸, L. Zhou^{1,a}, Li Zhou³⁰, X. Zhou⁵⁰, X. K. Zhou^{45,a}, X. R. Zhou^{45,a}, X. Y. Zhou¹, K. Zhu¹, K. J. Zhu^{1,a}, S. Zhu¹, X. L. Zhu³⁹, Y. C. Zhu^{45,a}, Y. S. Zhu¹, Z. A. Zhu¹, J. Zhuang^{1,a}, L. Zotti^{48A,48C}, B. S. Zou¹, J. H. Zou¹

(BESIII Collaboration)

¹ Institute of High Energy Physics, Beijing 100049, People's Republic of China

² Beihang University, Beijing 100191, People's Republic of China

³ Beijing Institute of Petrochemical Technology, Beijing 102617, People's Republic of China

⁴ Bochum Ruhr-University, D-44780 Bochum, Germany

⁵ Carnegie Mellon University, Pittsburgh, Pennsylvania 15213, USA

⁶ Central China Normal University, Wuhan 430079, People's Republic of China

⁷ China Center of Advanced Science and Technology, Beijing 100190, People's Republic of China

⁸ COMSATS Institute of Information Technology, Lahore, Defence Road, Off Raiwind Road, 54000 Lahore, Pakistan

⁹ G.I. Budker Institute of Nuclear Physics SB RAS (BINP), Novosibirsk 630090, Russia

¹⁰ GSI Helmholtzcentre for Heavy Ion Research GmbH, D-64291 Darmstadt, Germany

¹¹ Guangxi Normal University, Guilin 541004, People's Republic of China

¹² GuangXi University, Nanning 530004, People's Republic of China

- ¹³ Hangzhou Normal University, Hangzhou 310036, People's Republic of China
¹⁴ Helmholtz Institute Mainz, Johann-Joachim-Becher-Weg 45, D-55099 Mainz, Germany
¹⁵ Henan Normal University, Xinxiang 453007, People's Republic of China
¹⁶ Henan University of Science and Technology, Luoyang 471003, People's Republic of China
¹⁷ Huangshan College, Huangshan 245000, People's Republic of China
¹⁸ Hunan University, Changsha 410082, People's Republic of China
¹⁹ Indiana University, Bloomington, Indiana 47405, USA
²⁰ (A)INFN Laboratori Nazionali di Frascati, I-00044, Frascati, Italy; (B)INFN and University of Perugia, I-06100, Perugia, Italy
²¹ (A)INFN Sezione di Ferrara, I-44122, Ferrara, Italy; (B)University of Ferrara, I-44122, Ferrara, Italy
²² Johannes Gutenberg University of Mainz, Johann-Joachim-Becher-Weg 45, D-55099 Mainz, Germany
²³ Joint Institute for Nuclear Research, 141980 Dubna, Moscow region, Russia
²⁴ Justus Liebig University Giessen, II. Physikalisches Institut, Heinrich-Buff-Ring 16, D-35392 Giessen, Germany
²⁵ KVI-CART, University of Groningen, NL-9747 AA Groningen, Netherlands
²⁶ Lanzhou University, Lanzhou 730000, People's Republic of China
²⁷ Liaoning University, Shenyang 110036, People's Republic of China
²⁸ Nanjing Normal University, Nanjing 210023, People's Republic of China
²⁹ Nanjing University, Nanjing 210093, People's Republic of China
³⁰ Nankai University, Tianjin 300071, People's Republic of China
³¹ Peking University, Beijing 100871, People's Republic of China
³² Seoul National University, Seoul, 151-747 Korea
³³ Shandong University, Jinan 250100, People's Republic of China
³⁴ Shanghai Jiao Tong University, Shanghai 200240, People's Republic of China
³⁵ Shanxi University, Taiyuan 030006, People's Republic of China
³⁶ Sichuan University, Chengdu 610064, People's Republic of China
³⁷ Soochow University, Suzhou 215006, People's Republic of China
³⁸ Sun Yat-Sen University, Guangzhou 510275, People's Republic of China
³⁹ Tsinghua University, Beijing 100084, People's Republic of China
⁴⁰ (A)Istanbul Aydin University, 34295 Sefakoy, Istanbul, Turkey; (B)Dogus University, 34722 Istanbul, Turkey; (C)Uludag University, 16059 Bursa, Turkey
⁴¹ University of Chinese Academy of Sciences, Beijing 100049, People's Republic of China
⁴² University of Hawaii, Honolulu, Hawaii 96822, USA
⁴³ University of Minnesota, Minneapolis, Minnesota 55455, USA
⁴⁴ University of Rochester, Rochester, New York 14627, USA
⁴⁵ University of Science and Technology of China, Hefei 230026, People's Republic of China
⁴⁶ University of South China, Hengyang 421001, People's Republic of China
⁴⁷ University of the Punjab, Lahore-54590, Pakistan
⁴⁸ (A)University of Turin, I-10125, Turin, Italy; (B)University of Eastern Piedmont, I-15121, Alessandria, Italy; (C)INFN, I-10125, Turin, Italy
⁴⁹ Uppsala University, Box 516, SE-75120 Uppsala, Sweden
⁵⁰ Wuhan University, Wuhan 430072, People's Republic of China
⁵¹ Zhejiang University, Hangzhou 310027, People's Republic of China
⁵² Zhengzhou University, Zhengzhou 450001, People's Republic of China

^a Also at State Key Laboratory of Particle Detection and Electronics, Beijing 100049, Hefei 230026, People's Republic of China

^b Also at Ankara University, 06100 Tandoğan, Ankara, Turkey

^c Also at Bogazici University, 34342 Istanbul, Turkey

^d Also at the Moscow Institute of Physics and Technology, Moscow 141700, Russia

^e Also at the Functional Electronics Laboratory, Tomsk State University, Tomsk, 634050, Russia

^f Also at the Novosibirsk State University, Novosibirsk, 630090, Russia

^g Also at the NRC "Kurchatov Institute, PNPI, 188300, Gatchina, Russia

^h Also at University of Texas at Dallas, Richardson, Texas 75083, USA

ⁱ Present address: Istanbul Arel University, 34295 Istanbul, Turkey

We report an observation of the process $J/\psi \rightarrow \gamma X(1835) \rightarrow \gamma K_S^0 K_S^0 \eta$ at low $K_S^0 K_S^0$ mass with a statistical significance larger than 12.9σ using a data sample of 1.31×10^9 J/ψ events collected with the BESIII detector. In this region of phase space the $K_S^0 K_S^0$ system is dominantly produced through the $f_0(980)$. By performing a partial wave analysis, we determine the spin parity of the $X(1835)$ to be $J^{PC} = 0^{-+}$. The mass and width of the observed $X(1835)$ are $1844 \pm 9(\text{stat})^{+16}_{-25}(\text{syst})$ MeV/ c^2 and $192^{+20}_{-17}(\text{stat})^{+62}_{-43}(\text{syst})$ MeV, respectively, which are consistent with the results obtained by BESIII in the channel $J/\psi \rightarrow \gamma \pi^+ \pi^- \eta'$.

The non-Abelian property of quantum chromodynamics (QCD) permits the existence of bound states beyond conventional mesons and baryons, such as glueballs, hybrid states, and multiquark states. The search for these unconventional states is one of the main interests in experimental particle physics. One of the most promising candidates, the $X(1835)$ resonance, was first observed in its decay to $\pi^+\pi^-\eta'$ in the process $J/\psi \rightarrow \gamma\pi^+\pi^-\eta'$ by BESII [1]; this observation was subsequently confirmed by BESIII [2]. The discovery of the $X(1835)$ has stimulated theoretical speculation concerning its nature. Possible interpretations include a $p\bar{p}$ bound state [3], a second radial excitation of the η' [4], and a pseudoscalar glueball [5]. In addition, an enhancement in the invariant $p\bar{p}$ mass at threshold, $X(p\bar{p})$, was first observed by BESII in the decay $J/\psi \rightarrow \gamma p\bar{p}$ [6], and was later also seen by BESIII [7] and CLEO [8]. In a partial-wave analysis of $J/\psi \rightarrow \gamma p\bar{p}$, BESIII determined the J^{PC} of the $X(p\bar{p})$ to be 0^{-+} [9]. The mass of the $X(p\bar{p})$ is consistent with the $X(1835)$ mass measured in $J/\psi \rightarrow \gamma\pi^+\pi^-\eta'$ [2], but the width of the $X(p\bar{p})$ is significantly narrower.

To understand the nature of the $X(1835)$, it is crucial to measure its J^{PC} and to search for new decay modes. Because of its similarity to $J/\psi \rightarrow \gamma\pi^+\pi^-\eta'$, $J/\psi \rightarrow \gamma K\bar{K}\eta$ is a favorable channel to search for $X(1835) \rightarrow K\bar{K}\eta$. In contrast to $J/\psi \rightarrow \gamma K^+K^-\eta$, there is no background contamination for $J/\psi \rightarrow \gamma K_S^0 K_S^0 \eta$ from $J/\psi \rightarrow \pi^0 K_S^0 K_S^0 \eta$ and $J/\psi \rightarrow K_S^0 K_S^0 \eta$, which are forbidden by exchange symmetry and CP conservation. Therefore, the channel $J/\psi \rightarrow \gamma K_S^0 K_S^0 \eta$ provides a clean environment with minimal uncertainties due to background modeling. In this Letter, we report the first observation and spin-parity determination of the $X(1835)$ in $J/\psi \rightarrow \gamma K_S^0 K_S^0 \eta$, where the K_S^0 and η are reconstructed from their decays to $\pi^+\pi^-$ and $\gamma\gamma$, respectively. The analysis is based on a sample of $(1310.6 \pm 10.5) \times 10^6$ J/ψ events [10, 11] collected with the BESIII detector [12].

The BESIII detector is a magnetic spectrometer operating at BEPCII, a double-ring e^+e^- collider with center of mass energies between 2.0 and 4.6 GeV. The cylindrical core of the BESIII detector consists of a helium-based main drift chamber (MDC), a plastic scintillator time-of-flight system, and a CsI(Tl) electromagnetic calorimeter (EMC) that are all enclosed in a superconducting solenoidal magnet providing a 1.0 T (0.9 T in 2012, for about 1087×10^6 collected J/ψ) magnetic field. The solenoid is supported by an octagonal flux-return yoke with resistive plate counter muon identifier modules interleaved with steel. The acceptance of charged particles and photons is 93% of the 4π solid angle, and the charged-particle momentum resolution at 1 GeV/ c is 0.5%. The EMC measures photon energies with a resolution of 2.5% (5%) at 1 GeV in the barrel (end caps). A GEANT4-based [13] Monte Carlo (MC) simulation software package is used to optimize the event selection criteria, estimate backgrounds, and determine the detection efficiency.

Charged tracks are reconstructed using hits in the

MDC. Because there are two K_S^0 with displaced vertices, the point of closest approach of each charged track to the e^+e^- interaction point is required to be within ± 30 cm in the beam direction and within 40 cm in the plane perpendicular to the beam direction. The polar angle between the direction of a charged track and the beam direction must satisfy $|\cos\theta| < 0.93$. Photon candidates are selected from showers in the EMC with the energy deposited in the EMC barrel region ($|\cos\theta| < 0.8$) and the EMC end caps region ($0.86 < |\cos\theta| < 0.92$) greater than 25 MeV and 50 MeV, respectively. EMC cluster timing requirements are used to suppress electronic noise and energy deposits unrelated to the event.

Candidate $J/\psi \rightarrow \gamma K_S^0 K_S^0 \eta$ events are required to have four charged tracks with zero net charge and at least three photon candidates. All charged tracks are reconstructed under the pion hypothesis. To reconstruct K_S^0 candidates, the tracks of each $\pi^+\pi^-$ pair are fitted to a common vertex. K_S^0 candidates are required to satisfy $|M_{\pi^+\pi^-} - m_{K_S^0}| < 0.009$ GeV/ c^2 and $L/\sigma_L > 2$, where L and σ_L are the distance between the common vertex of the $\pi^+\pi^-$ pair and the primary vertex, and its error, respectively. The $\gamma\gamma\gamma K_S^0 K_S^0$ candidates are subject to a kinematic fit with four constraints (4C), ensuring energy and momentum conservation. Only candidates where the fit yields a χ^2_{4C} value less than 40 are retained for further analysis. For events with more than three photon candidates, multiple $J/\psi \rightarrow \gamma K_S^0 K_S^0 \eta$ candidates are possible. Only the combination yielding the smallest χ^2_{4C} is retained for further analysis. Candidate $J/\psi \rightarrow \gamma K_S^0 K_S^0 \eta$ events are required to have exactly one pair of photons within the η mass window ($0.51 < M_{\gamma\gamma} < 0.57$ GeV/ c^2). Simulation studies show this criterion significantly reduces the miscombination of photons from 3.20% to 0.16%. The miscombination of pions is also studied and found to be negligible. To further suppress background events containing a π^0 , events with any photon pair within a π^0 mass window ($0.10 < M_{\gamma\gamma} < 0.16$ GeV/ c^2) are rejected. The decay $J/\psi \rightarrow \phi K_S^0 K_S^0$ with $\phi \rightarrow \gamma\eta$ leads to the same final state as the investigated reaction $J/\psi \rightarrow \gamma K_S^0 K_S^0 \eta$. Therefore, events in the mass region $|M_{\gamma\eta} - m_\phi| < 0.04$ GeV/ c^2 are rejected.

After applying the selection criteria discussed above, the invariant mass spectrum of $K_S^0 K_S^0 \eta$ shown in Fig. 1 (a) is obtained. Besides a distinct η_c signal, a clear structure around 1.85 GeV/ c^2 is observed. The $K_S^0 K_S^0$ mass spectrum, shown in Fig. 1 (b), reveals a strong enhancement near the $K_S^0 K_S^0$ mass threshold, which is interpreted as the $f_0(980)$ by considering spin-parity and isospin conservation. The scatter plot of the invariant mass of $K_S^0 K_S^0$ versus that of $K_S^0 K_S^0 \eta$ is shown in Fig. 1 (c). A clear accumulation of events is seen around the intersection of the $f_0(980)$ and the structure around 1.85 GeV/ c^2 . This indicates that the structure around 1.85 GeV/ c^2 is strongly correlated with $f_0(980)$. By requiring $M_{K_S^0 K_S^0} < 1.1$ GeV/ c^2 , the structure around 1.85 GeV/ c^2 becomes much more prominent in the $K_S^0 K_S^0 \eta$ mass spectrum [Fig. 1 (d)]. In addition,

there is an excess of events around $1.6 \text{ GeV}/c^2$.

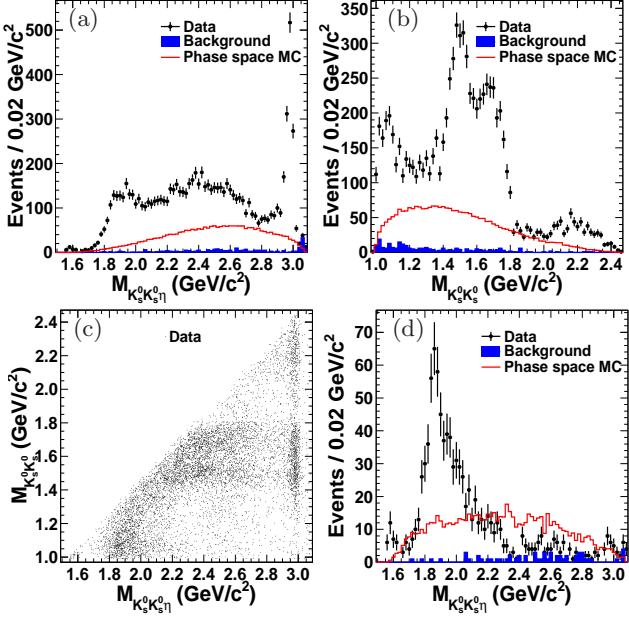


FIG. 1. Invariant mass distributions for selected events: Invariant mass spectra of (a) $K_S^0 K_S^0 \eta$ and (b) $K_S^0 K_S^0$; (c) scatter plot of $M_{K_S^0 K_S^0}$ versus $M_{K_S^0 K_S^0 \eta}$; (d) $K_S^0 K_S^0$ invariant mass spectrum for events with the requirement $M_{K_S^0 K_S^0} < 1.1 \text{ GeV}/c^2$. Dots with error bars are data; the shaded histograms are the non- η backgrounds estimated by the η sideband; the solid histograms are phase space MC events of $J/\psi \rightarrow \gamma K_S^0 K_S^0 \eta$ with arbitrary normalization.

Potential background processes are studied using a simulated sample of $1.2 \times 10^9 J/\psi$ decays, in which the decays with measured branching fractions are generated by EvtGEN [14] and the remaining J/ψ decays are generated according to the LUNDCHARM [15] model. Simulated events are subject to the same selection procedure applied to data. No significant peaking background sources have been identified in the invariant mass spectrum of $K_S^0 K_S^0 \eta$. Dominant backgrounds stem from $J/\psi \rightarrow \gamma K_S^0 K_S^0 \pi^0$ and $J/\psi \rightarrow \gamma K_S^0 K_S^0 \pi^0 \pi^0$. These non- η backgrounds are considered in the partial wave analysis (PWA) by selecting events from data in the η sideband regions defined as $0.45 < M_{\gamma\gamma} < 0.48 \text{ GeV}/c^2$ and $0.60 < M_{\gamma\gamma} < 0.63 \text{ GeV}/c^2$, and they account for about 2.5% of the total number of events in the η signal region.

A PWA of events satisfying $M_{K_S^0 K_S^0 \eta} < 2.8 \text{ GeV}/c^2$ and $M_{K_S^0 K_S^0} < 1.1 \text{ GeV}/c^2$ is performed to determine the parameters of the structure around $1.85 \text{ GeV}/c^2$. These restrictions reduce complexities due to additional intermediate processes. The signal amplitudes are parameterized as sequential two-body decays, according to the isobar model: $J/\psi \rightarrow \gamma X$, $X \rightarrow Y \eta$ or $Z K_S^0$, where Y and Z represent the $K_S^0 K_S^0$ and $K_S^0 \eta$ isobars, respectively. Parity conservation in the $J/\psi \rightarrow \gamma K_S^0 K_S^0 \eta$ decay restricts the possible J^{PC} of the $K_S^0 K_S^0 \eta$ (X) system to be 0^{-+} , 1^{++} , $2^{++}, 2^{-+}$, 3^{++} , etc.

In this Letter, only spins $J < 3$ and possible S -wave or P -wave decays of the X are considered. The amplitudes are constructed using the covariant tensor formalism described in Ref. [16]. The relative magnitudes and phases of the partial wave amplitudes are determined by an unbinned maximum likelihood fit to data. The contribution of non- η background events is accounted for in the fit by subtracting the negative log-likelihood (NLL) value obtained for events in the η sideband region from the NLL value obtained for events in the η signal region. The statistical significance of a contribution is estimated by the difference in NLL with and without the particular contribution, taking the change in degrees of freedom into account.

Our initial PWA fits include an $X(1835)$ resonance in the $f_0(980)\eta$ channel and a nonresonant component in one of the possible decay channels $f_0(980)\eta$, $f_0(1500)\eta$ or $f_2(1525)\eta$. All possible J^{PC} combinations of the $X(1835)$ and the nonresonant component are tried. We then extend the fits by including an additional resonance at lower $K_S^0 K_S^0 \eta$ mass. This additional component, denoted here as the $X(1560)$, improves the fit quality when it is allowed to interfere with the $X(1835)$. Our final fits show that the data can be best described with three components: $X(1835) \rightarrow f_0(980)\eta$, $X(1560) \rightarrow f_0(980)\eta$, and a nonresonant $f_0(1500)\eta$ component. The J^{PC} of the $X(1835)$, the $X(1560)$, and the nonresonant component are all found to be 0^{-+} . The $X(1835)$, $X(1560)$, and $f_0(1500)$ are described by nonrelativistic Breit-Wigner functions, where the intrinsic widths are not energy dependent. The masses and widths of the $X(1835)$ and $X(1560)$ are derived by scanning each over a certain range. The $f_0(1500)$ mass and width are fixed to the values reported in Ref. [17]. The $f_0(980)$ is parameterized by the Flatté formula [18], with the parameters fixed to the values reported by BESII [19] in the channels $J/\psi \rightarrow \phi \pi^+ \pi^-$ and $J/\psi \rightarrow \phi K^+ K^-$. The scan returns a mass and width of the $X(1835)$ of $1844 \pm 9 \text{ MeV}/c^2$ and $192^{+20}_{-17} \text{ MeV}$, respectively. The mass and width of the $X(1560)$ are determined to be $1565 \pm 8 \text{ MeV}/c^2$ and $45^{+14}_{-13} \text{ MeV}$, respectively. Using a detection efficiency of 5.5%, obtained by a MC sample weighted by partial wave amplitudes, the product branching fraction of $J/\psi \rightarrow \gamma X(1835)$ and $X(1835) \rightarrow K_S^0 K_S^0 \eta$ ($\mathcal{B}_{X(1835)}$) is calculated to be $(3.31^{+0.33}_{-0.30}) \times 10^{-5}$, where the decay $X(1835) \rightarrow K_S^0 K_S^0 \eta$ is dominated by $f_0(980)$ production. The $K_S^0 K_S^0 \eta$, $K_S^0 K_S^0$, $K_S^0 \eta$ mass spectra and the distributions of the J/ψ , $K_S^0 K_S^0 \eta$ and $K_S^0 K_S^0$ decay angles are shown in Fig. 2. Overlaid on the data are the PWA fit projections, as well as the individual contributions from each component. The χ^2/n_{bin} value is displayed on each figure to demonstrate the goodness of fit. We evaluate the significance by applying the likelihood ratio test, performing a separate fit for every systematic variation detailed below. The most conservative statistical significances of the $X(1835)$ and $X(1560)$ are 12.9σ and 8.9σ , respectively.

Various fits are performed by changing the J^{PC} and

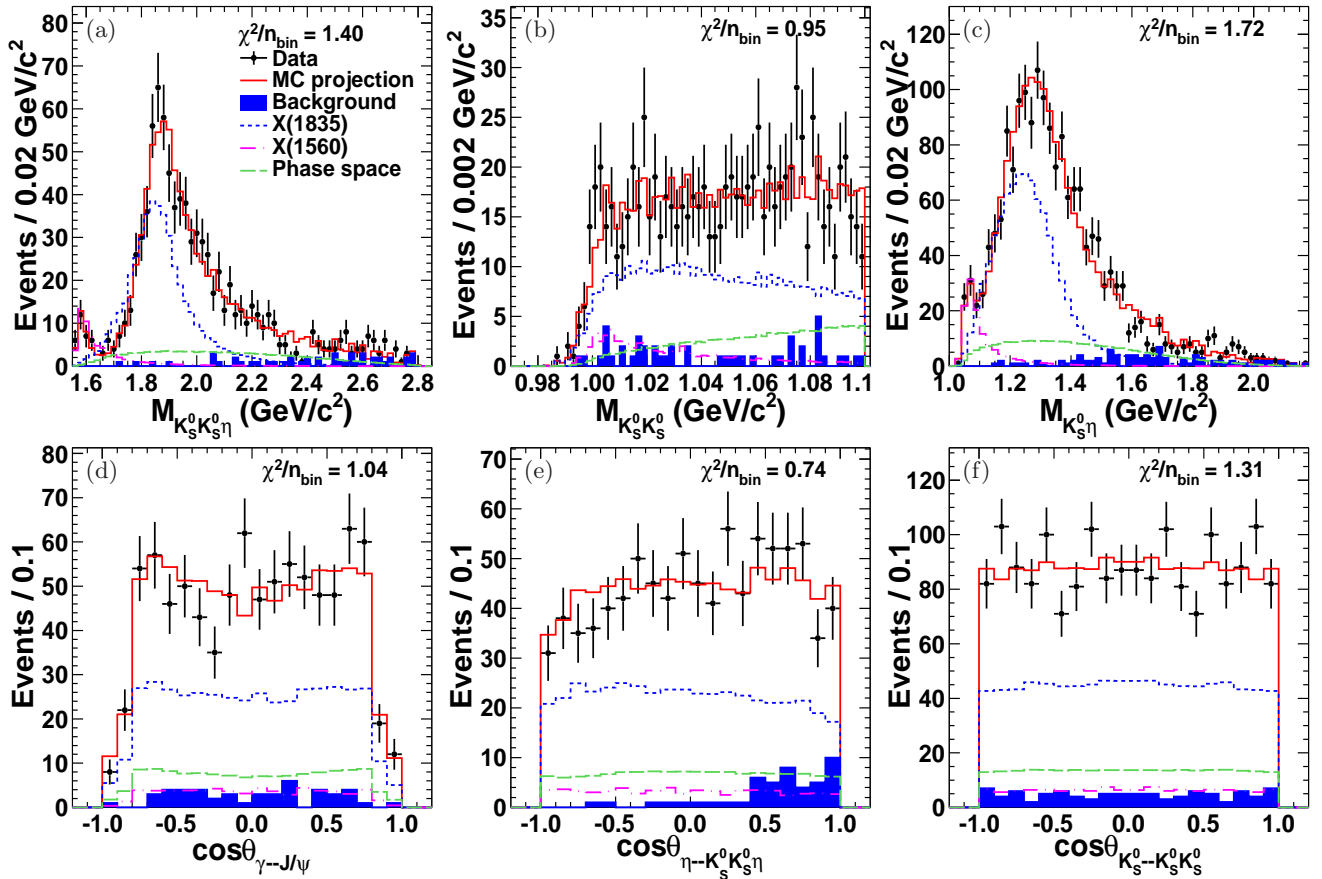


FIG. 2. Comparisons between data and PWA fit projections. (a), (b), and (c) are the invariant mass distributions of $K_S^0 K_S^0 \eta$, $K_S^0 K_S^0$, and $K_S^0 \eta$ (two entries/event), respectively. (d)-(f) are the angular distributions of $\cos \theta$, where θ is the polar angle of (d) γ in the J/ψ rest system; (e) η in the $K_S^0 K_S^0 \eta$ rest system; and (f) K_S^0 in the $K_S^0 K_S^0$ rest system (two entries/event). The dots with error bars are data, the solid histograms are the PWA total projections, the shaded histograms are the non- η backgrounds estimated by the η sideband, and the short-dashed, dash-dotted, and long-dashed histograms show the contributions of $X(1835)$, $X(1560)$, and the nonresonant component, respectively.

decay mode of the nonresonant component compared to the nominal solution described above. The NLL value of a fit with a 1^{++} nonresonant $f_0(1500)\eta$ component is only worse by 0.8 compared to the nominal solution, which indicates that we cannot distinguish between the two spin assignments of the nonresonant component with our present statistics. This ambiguity introduces large systematic uncertainties in the $\mathcal{B}_{X(1835)}$, since the interference between the $X(1835)$, $X(1560)$, and the nonresonant component depends on the spin assignment of the latter. To establish the J^{PC} of the $X(1835)$, we perform a series of PWA fits assuming alternative J^{PC} hypotheses for both the $X(1835)$ and the nonresonant contribution. For the nonresonant contribution, we also test several possible decay channels [$f_0(980)\eta$, $f_0(1500)\eta$, and $f_2(1525)\eta$] in turn. For each nonresonant component assumption, the $X(1835) 0^{-+}$ hypothesis is significantly better than the 1^{++} or 2^{-+} hypotheses, with the NLL value improving by at least 41.6 units. Analogously, we perform the same series of PWA fits for the $X(1560)$. Again the 0^{-+} hypothesis for the $X(1560)$ always yields

a significantly better fit result than other J^{PC} assignments, with the NLL value improving by at least 12.8 units.

We evaluate the contributions from additional well-known resonances by adding them individually to the fit. We consider all possible combinations for X and its subsequent decay products Y and Z as given in Ref. [17]: for X , this includes $\eta(1760)$, $\eta(2225)$, $f_1(1510)$, $\eta_2(1870)$, $f_2(1810)$, $f_2(1910)$, $f_2(1950)$, $f_2(2010)$, $f_2(2150)$, $f_2(2300)$, $f_2(2340)$, $f_J(2220)$; for Y , $f_0(980)$, $f_0(1500)$, $f_0(1710)$, $f_2(1270)$ and $f_2(1525)$; for Z , $K^*(1410)$, $K^*(1680)$, $K_0^*(1430)$, $K_0^*(1950)$, $K_2^*(1430)$, and $K_2^*(1980)$. Additional nonresonant contributions with various J^{PC} and decay modes are studied as well. The statistical significances of the additional contributions are smaller than 5σ . In order to check the possible contribution from a nonresonant $K_S^0 K_S^0$ process, we add a $X(1835) \rightarrow (K_S^0 K_S^0)_S \eta$ process into the nominal solution, where $(K_S^0 K_S^0)_S$ refers to a nonresonant $K_S^0 K_S^0$ contribution in a relative S wave. We find the resulting significance of the $X(1835) \rightarrow f_0(980)\eta$ pro-

cess and the $X(1835) \rightarrow (K_S^0 K_S^0)S\eta$ process to be 6.8σ and 1.6σ , respectively, so we do not include the latter process in the nominal solution. We also test a fit by changing the decay mode of the $X(1560)$ in the nominal solution from $f_0(980)\eta$ to $(K_S^0 K_S^0)S\eta$; the fit with $X(1560) \rightarrow (K_S^0 K_S^0)S\eta$ has almost the same fit quality as the nominal solution. Therefore, with the present statistics, we cannot draw a conclusion about the $X(1560)$ decay mode. The largest differences in masses and widths of the $X(1835)$ and $X(1560)$ and the product branching fraction $\mathcal{B}_{X(1835)}$ between all above alternative fits and the nominal solution are taken as systematic uncertainties from the components in the nominal solution.

For the measurements of the masses and widths of the $X(1835)$ and $X(1560)$ and the product branching fraction $\mathcal{B}_{X(1835)}$, we include the following sources of systematic uncertainties in addition to the sources discussed above: we change the $K_S^0 K_S^0$ mass range to $M_{K_S^0 K_S^0} < 1.05, 1.15$ and $1.20 \text{ GeV}/c^2$; we change the $f_0(980)$ mass and coupling constants in the Flatté formula to other experimental measurements [20–22]; we change the $f_0(1500)$ mass and width by one standard deviation [17]; we increase and decrease the non- η background level by one standard deviation; we change the parameterization of the $X(1835)$ and $X(1560)$ line shape to a Breit-Wigner function whose intrinsic width is energy-dependent [23]; and we replace the $X(1560)$ by $\eta(1405)$ or $\eta(1475)$. For the systematic errors of the product branching fraction $\mathcal{B}_{X(1835)}$, we also consider the following additional uncertainties. The K_S^0 reconstruction efficiency is studied using two control samples of $J/\psi \rightarrow K^{\pm} K^{\mp}$ and $J/\psi \rightarrow \phi K_S^0 K^{\pm} \pi^{\mp}$, while the photon detection efficiency is investigated based on a clean sample of $J/\psi \rightarrow \rho\pi$. The differences between data and MC simulation are 1.0% for each K_S^0 and 1.0% for each photon [24]. A control sample of $J/\psi \rightarrow \gamma K_S^0 K_S^0 \pi^0$ is selected to estimate the uncertainty associated with the 4C kinematic fit. The efficiency is the ratio of the signal yields with and without the kinematic fit requirement $\chi_{4C}^2 < 40$. The difference between data and MC simulation, 1.5%, is assigned as the systematic uncertainty. We also consider the uncertainties from the number of J/ψ events [10, 11] and the branching fractions of $K_S^0 \rightarrow \pi^+ \pi^-$ and $\eta \rightarrow \gamma\gamma$ [17]. We change the mass and width of $X(1835)$ or $X(1560)$ by 1 standard deviation of the statistical uncertainty. The individual uncertainties are assumed to be independent and are added in quadrature to obtain the total systematic uncertainties as presented in the Supplemental Material [25].

In summary, a PWA of $J/\psi \rightarrow \gamma K_S^0 K_S^0 \eta$ has been performed in the mass range $M_{K_S^0 K_S^0 \eta} < 2.8 \text{ GeV}/c^2$ after requiring $M_{K_S^0 K_S^0} < 1.1 \text{ GeV}/c^2$. The PWA fit requires a contribution from $X(1835) \rightarrow K_S^0 K_S^0 \eta$ with a statistical significance greater than 12.9σ , where the $X(1835) \rightarrow K_S^0 K_S^0 \eta$ is dominated by $f_0(980)$ produc-

tion. The spin parity of the $X(1835)$ is determined to be 0^{-+} . The mass and width of the $X(1835)$ are measured to be $1844 \pm 9(\text{stat})^{+16}_{-25}(\text{syst}) \text{ MeV}/c^2$ and $192^{+20}_{-17}(\text{stat})^{+62}_{-43}(\text{syst}) \text{ MeV}$, respectively. The corresponding product branching fraction $\mathcal{B}_{X(1835)}$ is measured to be $(3.31^{+0.33}_{-0.30}(\text{stat})^{+1.96}_{-1.29}(\text{syst})) \times 10^{-5}$. The mass and width of the $X(1835)$ are consistent with the values obtained from the decay $J/\psi \rightarrow \gamma\pi^+\pi^-\eta'$ by BESIII [2]. These results are all first-time measurements and provide important information to further understand the nature of the $X(1835)$.

Another 0^{-+} state, the $X(1560)$, also is observed in data with a statistical significance larger than 8.9σ and is seen to interfere with the $X(1835)$. The mass and width of the $X(1560)$ are determined to be $1565 \pm 8(\text{stat})^{+0}_{-63}(\text{syst}) \text{ MeV}/c^2$ and $45^{+14}_{-13}(\text{stat})^{+21}_{-28}(\text{syst}) \text{ MeV}$, respectively. The mass and width of the $X(1560)$ are consistent with those of the $\eta(1405)$ and $\eta(1475)$ as given in Ref. [17] within 2.0σ and 1.4σ , respectively. Present statistics do not allow us to conclusively determine if the $X(1560)$ is the same state as the $\eta(1405)/\eta(1475)$ or a new meson. More statistics in this analysis and an amplitude analysis of $J/\psi \rightarrow \gamma\eta\pi^0\pi^0$ and $J/\psi \rightarrow \gamma K_S^0 K_S^0 \pi^0$ processes may help to understand the nature of the $X(1560)$.

The BESIII collaboration thanks the staff of BEPCII and the IHEP computing center for their strong support. This work is supported in part by National Key Basic Research Program of China under Contract No. 2015CB856700; National Natural Science Foundation of China (NSFC) under Contracts No. 11125525, No. 11235011, No. 11322544, No. 11335008, No. 11425524; the Chinese Academy of Sciences (CAS) Large-Scale Scientific Facility Program; the CAS Center for Excellence in Particle Physics (CCEPP); the Collaborative Innovation Center for Particles and Interactions (CICPI); Joint Large-Scale Scientific Facility Funds of the NSFC and CAS under Contracts No. 11179007, No. U1232201, No. U1332201; CAS under Contracts No. KJCX2-YW-N29, No. KJCX2-YW-N45; 100 Talents Program of CAS; INPAC and Shanghai Key Laboratory for Particle Physics and Cosmology; German Research Foundation DFG under Contract No. Collaborative Research Center CRC-1044; Istituto Nazionale di Fisica Nucleare, Italy; Ministry of Development of Turkey under Contract No. DPT2006K-120470; Russian Foundation for Basic Research under Contract No. 14-07-91152; U.S. Department of Energy under Contracts No. DE-FG02-04ER41291, No. DE-FG02-05ER41374, No. DE-FG02-94ER40823, No. DESC0010118; U.S. National Science Foundation; University of Groningen (RuG) and the Helmholtzzentrum fuer Schwerionenforschung GmbH (GSI), Darmstadt; WCU Program of National Research Foundation of Korea under Contract No. R32-2008-000-10155-0.

-
- [1] M. Ablikim *et al.* (BES Collaboration), Phys. Rev. Lett. **95**, 262001 (2005).
- [2] M. Ablikim *et al.* (BESIII Collaboration), Phys. Rev. Lett. **106**, 072002 (2011).
- [3] S. L. Zhu and C. S. Gao, Commun. Theor. Phys. **46**, 291 (2006); J. P. Dedonder, B. Loiseau, B. El-Bennich, and S. Wycech, Phys. Rev. C **80**, 045207 (2009); G. J. Ding, R. G. Ping, and M. L. Yan, Eur. Phys. J. A **28**, 351 (2006); C. Liu, Eur. Phys. J. C **53**, 413 (2008); Z. G. Wang and S. L. Wan, J. Phys. G**34**, 505 (2007).
- [4] T. Huang and S. L. Zhu, Phys. Rev. D **73**, 014023 (2006).
- [5] N. Kochelev and D. P. Min, Phys. Lett. B **633**, 283 (2006); G. Hao, C. F. Qiao, and A. Zhang, Phys. Lett. B **642**, 53 (2006); B. A. Li, Phys. Rev. D **74**, 034019 (2006).
- [6] J. Z. Bai *et al.* (BES Collaboration), Phys. Rev. Lett. **91**, 022001 (2003).
- [7] M. Ablikim *et al.* (BESIII Collaboration), Chin. Phys. C **34**, 421 (2010).
- [8] J. P. Alexander *et al.* (CLEO Collaboration), Phys. Rev. D **82**, 092002 (2010).
- [9] M. Ablikim *et al.* (BESIII Collaboration), Phys. Rev. Lett. **108**, 112003 (2012).
- [10] M. Ablikim *et al.* (BESIII Collaboration), Chin. Phys. C **36**, 915 (2012).
- [11] With the same approach as in Ref. [10], the preliminary number of J/ψ events taken in 2009 and 2012 is determined to be 1310.6×10^6 with an uncertainty of 0.8%.
- [12] M. Ablikim *et al.* (BESIII Collaboration), Nucl. Instrum. Meth. Phys. Res., Sect. A **614**, 345 (2010).
- [13] S. Agostinelli *et al.* (GEANT4 Collaboration), Nucl. Instrum. Meth. Phys. Res., Sect. A **506**, 250 (2003).
- [14] D. J. Lange, Nucl. Instrum. Meth. Phys. Res., Sect. A **462**, 152 (2001); R. G. Ping, Chin. Phys. C **32**, 599 (2008).
- [15] J. C. Chen, G. S. Huang, X. R. Qi, D. H. Zhang, and Y. S. Zhu, Phys. Rev. D **62**, 034003 (2000).
- [16] B. S. Zou and D. V. Bugg, Eur. Phys. J. A **16**, 537 (2003).
- [17] K. A. Olive *et al.* (Particle Data Group), Chin. Phys. C **38**, 090001 (2014).
- [18] S. M. Flatté, Phys. Lett. **63B**, 224 (1976).
- [19] M. Ablikim *et al.* (BES Collaboration), Phys. Lett. B **607**, 243 (2005).
- [20] M. N. Achasov *et al.*, Phys. Lett. B **485**, 349 (2000).
- [21] A. Aloisio *et al.* (KLOE Collaboration), Phys. Lett. B **537**, 21 (2002).
- [22] B. S. Zou and D. V. Bugg, Phys. Rev. D **48**, R3948 (1993).
- [23] J. H. Kühn and A. Santamaria, Z. Phys. C **48**, 445 (1990).
- [24] M. Ablikim *et al.* (BESIII Collaboration), Phys. Rev. D **81**, 052005 (2010).
- [25] See Supplemental Material at <http://link.aps.org/supplemental/10.1103/PhysRevLett.115.091803> for the summary of systematic uncertainties for the measurements of masses, widths of the $X(1835)$ and $X(1560)$, and the product branching fraction $\mathcal{B}_{X(1835)}$.